Proceedings of the 48th International School and Conference on the Physics of Semiconductors "Jaszowiec 2019"

Magnetic and Structural Properties of ZnO Implanted with Co, Kr, and Ar Ions

J.B. Gosk[a,*], Z. Werner[b], G. Kowalski[c], M. Tokarczyk[c], R. Puźniak[d], and M. Barlak[b]

[a]Faculty of Physics, Warsaw University of Technology, Koszykowa 75, PL-00662 Warsaw, Poland
[b]Nuclear Centre for Research, A. Sołtana 7, PL-05400 Otwock, Poland
[c]Institute of Experimental Physics, Faculty of Physics, University of Warsaw, L. Pasteura 5, PL-02093 Warsaw, Poland
[d]Institute of Physics, Polish Academy of Sciences, Aleja Lotnikow 32/46, PL-02668 Warsaw, Poland

Studies of structural and magnetic properties of Co-, Kr-, and Ar-implanted ZnO were performed by means of X-ray diffraction and SQUID magnetometry. Magnetization was measured at the same conditions prior and after implantation. For each kind of applied ions, implantation was carried out for two selected, as a result of preliminary calculations, fluences. In Co implanted ZnO, thin layer magnetization measurements revealed the appearance of the Brillouin-kind paramagnetic phase accompanied by some residual ferromagnetic/superparamagnetic contribution. The magnetic moment equal to about 1.7 μ_B per implanted Co ion in the case of implantation with higher dose of 4×10^{16} cm^{-2} and about 2.1 μ_B in the case of implantation with lower dose of 2×10^{16} cm^{-2} Co ions was observed. On the other hand, no changes in magnetization were observed as a result of implantation for Kr- or Ar-implanted ZnO. Thus, we could not find any evidence that irradiation damages caused by Kr and Ar ions, in the range of ion energies and fluences used by us, could result in magnetic response.

DOI: 10.12693/APhysPolA.136.628
PACS/topics: 61.05.cp, 75.30.Hx, 75.50.Pp, 82.80.Yc, 85.40.Ry

1. Introduction

Zinc oxide, ZnO, a wide bandgap semiconductor has been intensively investigated in the last decades by experimentalists, technologists, and theoreticians due to its possible application in optoelectronic devices such as solar cells, ultraviolet emitting diodes, and transparent high-power electronic devices. Recently, ZnO suitably doped with cobalt was considered as a potential and promising candidate for spintronics applications. However, the results of numerous implantation studies often contradict each other because of a lack of agreement on the origin of created magnetic units. It is frequently concluded that the implantation defects rather than the transition metal (TM) impurities give rise to the observed magnetization [1, 2]. It was suggested that ferromagnetic (FM) or paramagnetic (PM) phase, observed in ZnO, is either entirely defect related or appearing due to an interaction between defects and implantation-introduced impurities, including those without magnetic moments [2-6]. Since there are reports which attribute magnetic properties to the irradiation created defects like V_{Zn} [2], in our previous publication [7] we attempted to disclose PM/FM phase in ZnO samples containing no TM impurity but only defects. In the previous studies, we irradiated the ZnO bulk samples with electrons, protons, and Co ions. However, only Co implanted ZnO revealed PM phase introduced by irradiation and we concluded that defects created by electrons and protons are magnetically inactive.

It can be argued that defects caused by the action of electrons and protons are in fact insufficient to reproduce the desired magnetic properties of heavy ion defects accompanying cobalt implantation. Hence, as the next step in explaining what might be responsible for the existence of the paramagnetic phase in ZnO, i.e., to distinguish between the impact of post implantation defects or TM or maybe the presence of both at the same time, we decided to compare magnetic properties of ZnO implanted with heavy ions of similar mass, but differing in terms of magnetic moments. The aim of this study is to compare magnetic properties of ZnO implanted with Co, Ar (a noble gas lighter than Co), and Kr (a noble gas heavier than Co).

2. Samples

To determine the energy of Ar and Kr ions producing appropriate damage ranges, i.e., identical with that relevant to 110 keV Co in ZnO, the SUSPRE code [8] was used. In turn, to establish the appropriate dose, we calculated the amount of energy transferred to the lattice by 110 keV Co beam with fluence of 2×10^{16} cm^{-2} and we calculated appropriate Ar and Kr fluences carrying identical amount of energy. No correction for sputtering

*corresponding author; e-mail: gosk@fuw.edu.pl

was made as we assumed that ions so close to each other in mass exhibit similar sputtering yields. The results of calculations are collected in Table I.

TABLE I

Ions, energies, and doses applied in the experiment with Co-, Kr-, and Ar- implantation. The sample label prior and after implantation for each applied dose is given in Table.

Ion	Energy [keV]	Dose I [10^{16} cm^{-2}]	Dose II [10^{16} cm^{-2}]
Co	110	2.00 (Vir #1 vs. ZnO Co #1)	4.00 (Vir #5 vs. ZnO Co #5)
Ar	70	3.14 (Vir #2 vs. ZnO Ar #2)	6.30 (Vir #3 vs. ZnO Ar #3)
Kr	160	1.37 (Vir #4 vs. ZnO Kr #4)	2.75 (Vir #6 vs. ZnO Kr #6)

Plates in the form of 5×5 mm^2, were prepared from commercial Mateck ZnO single crystals of [100] orientation; each sample consisted of two such squared plates. In total six samples were implanted (with ions, energies, and doses indicated in Table I) at 500 keV implanter at HZDR, Rossendorf, Germany. For each selected ion, its energy, and dose the two plates were implanted, one of them shielded in one half by silicon screen to preserve a virgin material for the Rutherford backscattering (RBS). Utmost care was taken to avoid sample contact with metal tools. For this purpose the samples were mounted on silicon targets. Prior and after implantation, the sample magnetization was measured. To increase magnetic signal from thin investigated layers, two square plates were implanted with identical dose and they were stuck together with nonmagnetic glue during magnetization measurements. Since only one half of the second sample is implanted (see above), the total surface of the measured sample amounts to 0.375 cm^2 ($0.5 \times 0.5 + \frac{1}{2} \cdot 0.5 \times 0.5$ cm^2). After magnetic measurements, RBS spectra were recorded for all samples in random and aligned orientations, using 1.7 MeV He^+ ions. The spectra show that the damage in ion implanted ZnO is incomplete and does not convert the sample into amorphous, as deduced from the fact that the aligned spectra have lower intensity than the random ones. The details of RBS measurements will be presented elsewhere.

3. Results and discussion

3.1. X-ray diffraction measurements

X-ray diffraction measurements were based on X'pert Phillips Diffractometer equipped with standard laboratory X-ray source (CuK_α radiation) and Bartels type 4-crystal monochromator as a beam source. Diffracted beam optics comprised of 2-crystal analyzer and standard slit system. Two types of scans were performed: so called diffractometric $2\theta/\omega$ scan allowing for recording crystal interplanar spacing changes and ω scan which records the Bragg planes tilts both for chosen X-ray symmetric reflection. We investigated ZnO (002) Bragg planes parallel to the main (001) sample crystal surfaces. All the scans were performed in step scan mode with angular steps of either 0.001 or 0.002 deg.

The results for implanted samples were compared with those for unimplanted ZnO samples scanned in the same two modes $2\theta/\omega$ and ω. Our scans are effectively illustrating either crystal lattice interplanar spacing differences compared to the standard d_{hkl} value and tilts compared to the standard position of the (hkl) plane in symmetric reflection, respectively. Position and shape of implanted crystal scan recording have to be taken into account when comparing with scans of unimplanted sample. Since the observed lattice distortions and defects produced by implantation, reflected as differences between the recorded curves in comparison to the bare substrate recording, are relatively small, as compared to the maximum values in the peaks, we have chosen the logarithmic scale for intensity. Characteristically, since the unimplanted sample recordings ($2\theta/\omega$ and ω) are both symmetric, differences are easily seen as asymmetry for implanted samples in Figs. 1 and 2. One has to bear in mind that this type of experiment probes the whole volume of the sample and depth information is lost.

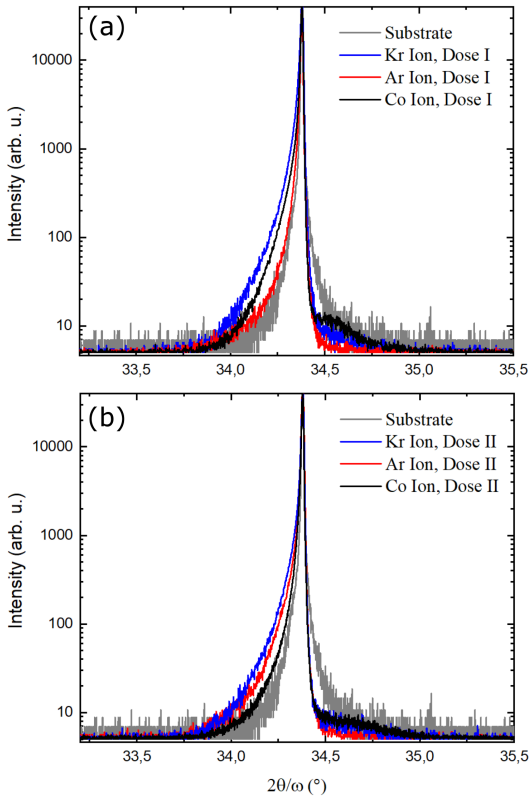

Fig. 1. $2\theta/\omega$ scans for the samples with three implants (Kr, Co, and Ar) for two doses: dose I (a) and dose II (b).

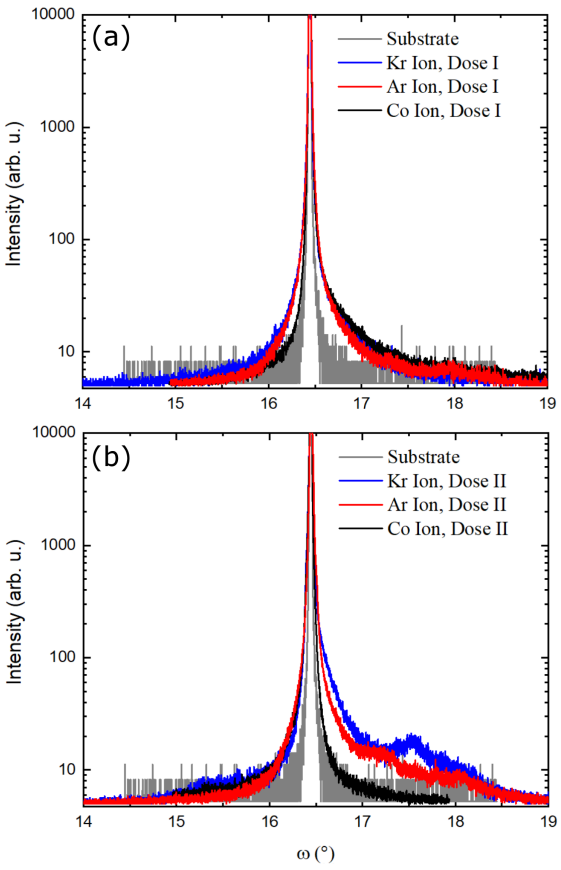

Fig. 2. ω scans for the samples with three implants (Co, Ar and Kr) for two doses: dose I (a) and dose II (b).

Figure 1 shows clearly that both doses caused similar asymmetry and shift of distribution to lower angles indicating rise of interplanar spacing in the region affected by implantation. Cobalt ion spectrum has also unexpected bump in the higher angles as if the lattice has slightly collapsed by the damage locally.

Figure 2 has basically shown difference between the effect of the dose I and II implantation with the dose II significantly more disturbing the lattice planes and tilting them with respect to the unimplanted sample towards the one side. This can be seen as evident asymmetry in distribution on higher angle side. Again Co ions are standing out in those figures with the dose I prevailing to dose II. The scan for the sample with dose II for Co is unexpectedly almost similar to that one of unimplanted sample.

3.2. Magnetization

Magnetization of the studied samples was measured as a function of magnetic field (M vs. H) at different temperatures in the field range from to 70 kOe and as a function of temperature (M vs. T) at $H = 1$ kOe and $H = 1$ kOe in the temperature range from 2 to 300 K using a SQUID MPMS XL.

3.2.1. Unimplanted ZnO samples

The results of our previous measurements performed on bulk Co-implanted ZnO revealed two facts, which we had to take into consideration. Firstly, the thin layer contribution in total magnetization of ZnO implanted with Co ions was significantly smaller than the dominant diamagnetic one of the ZnO lattice and secondly, it was only twice as large as the paramagnetic contribution (PM) originated from magnetic impurities of the parent ZnO. To increase the magnetic signal, the samples consisted of two squares plates. Each sample with the highest accuracy was centrally glued in the diamagnetic straws. All samples were measured before and after implantation at the same magnetic fields and temperatures. Thus, we could correct magnetization of all implanted ZnO samples for the magnetization of relevant parent ZnO. However, it should be noticed that small differences in sample mounting can result in a change of few percent of the total measured moment. Since the diamagnetic signal largely dominates, the curve resulting from the subtraction (magnetization of implanted and non-implanted samples) would be affected by an erroneous linear component.

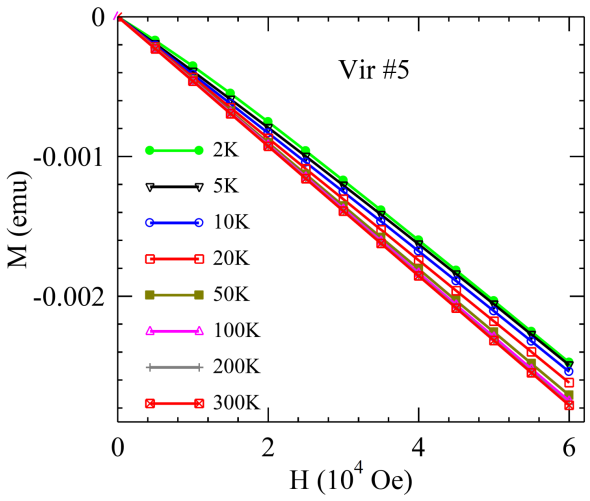

Fig. 3. Magnetization as a function of magnetic field recorded at different temperatures for the unimplanted sample Vir #5.

All measured ZnO unimplanted/reference samples (denoted in Figs. 3–4, and Fig. 6 as Vir #1–Vir #6) reveal the expected dominant diamagnetic contribution, in the total magnetization, accompanied by much weaker but still pronounced PM one. Figure 3 shows M vs. H for ZnO — Vir #5, which is representative of all virgin samples. Generally, between the six referential ZnO samples the differences in the measured magnetization were not observed. This is demonstrated by collected data presenting M vs. T at $H = 10$ kOe in Fig. 4. The experimental points for Vir #2, Vir #3, Vir #4, and Vir #6 practically overlap. Small differences in the position of the curves result mainly from not imperfect centric glu-

ing of the samples to the straws and slightly different sample masses. The M vs. T curves at $H = 1$ kOe (not shown, with the exception of Vir #5 displayed in Fig. 6b) of the six virgin samples measured at $H = 1$ kOe curves practically overlap. The lack of differences of magnetic properties between reference ZnO samples also results from M vs. H measurements (not shown).

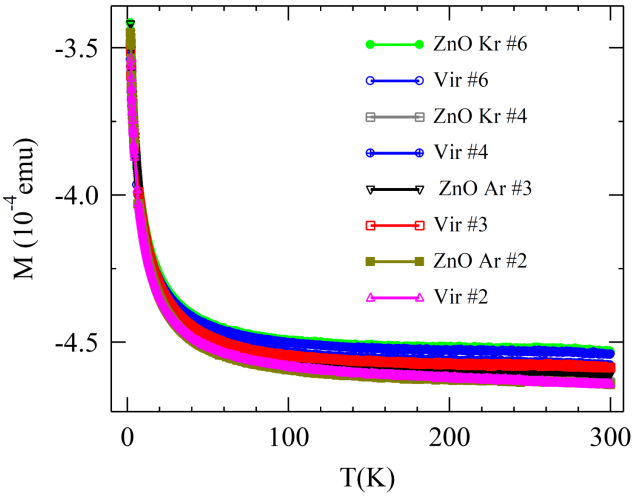

Fig. 4. Collected magnetization data obtained as a function of temperature at $H = 10$ kOe for the Ar- and Kr-implanted ZnO samples with dose I (ZnO Ar #2, ZnO Kr #4) and with dose II (ZnO Ar #3, ZnO Kr #6) compared with the data for relevant virgin samples (dose I: Vir #2, Vir #4; dose II: Vir #3, Vir #6).

3.2.2. Implanted ZnO

To compare magnetic properties of reference ZnO with Ar- and Kr-implanted ZnO (dose I and dose II), the H vs. T curves of two groups were placed in Fig. 4. It clearly shows that there is no effect of Kr- or Ar-ions implantation on magnetic properties of the ZnO. The M vs. H measurements (not shown) of Ar- and Kr-implanted ZnO confirm the statement; the M vs. H curves (at 2, 5, 10, 20, 50, 100, 200, and 300 K) of relevant Ar- and Kr- implanted ZnO and virgin ZnO samples practically overlap.

On the contrary, a significant change in magnetic properties was observed in Co-implanted ZnO magnetization measured as a function of the magnetic field at different temperatures for the sample ZnO Co #5 (dose II) after correction (subtraction of magnetization of the two relevant samples) for parent ZnO (Vir #5) contribution is depicted in Fig. 5.

In general, the presented data show a typical PM behavior. At low temperatures (e.g., 2 K), the magnetization reveals a pronounced tendency to saturate with increase of magnetic field while at high temperatures ($T > 50$ K) the magnetization is, practically, a linear function of the magnetic field. As readily seen, at low temperatures ($T \leq 50$ K) some additional residual phase manifests itself by rapid increase of magnetization at low

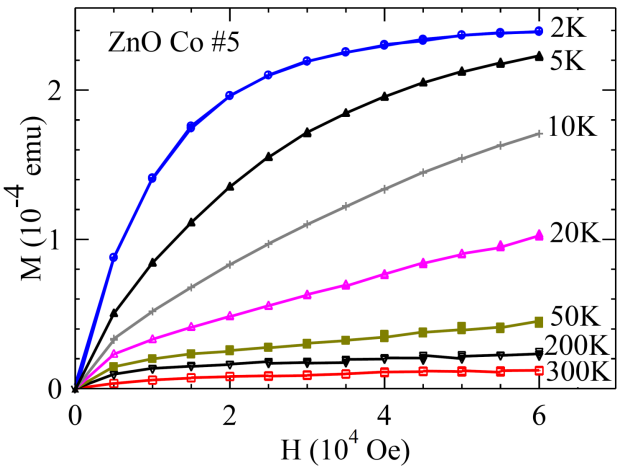

Fig. 5. Magnetization as a function of magnetic field at different temperatures for ZnO Co #5 sample, corrected for parent ZnO sample contribution (see, the text).

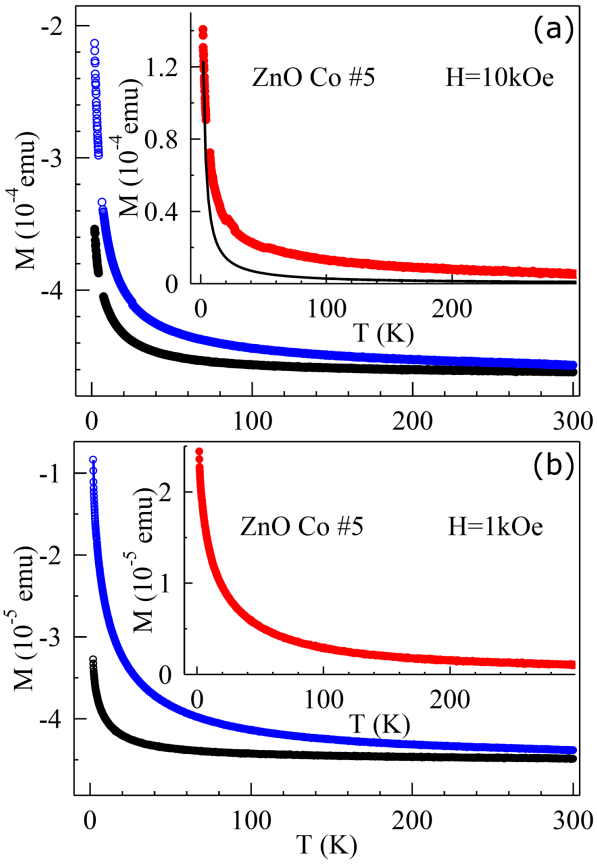

Fig. 6. Magnetization as a function of temperature for ZnO Co #5 — the blue points and for virgin sample Vir #5 — the black points, measured at (a) $H = 10$ kOe and (b) at $H = 1$ kOe. The results of subtraction the magnetization of referential sample from magnetization of Co-implanted ZnO — red points, are shown in the insets. The black line in the inset of Fig. 6a represents the Brillouin function (see the text).

magnetic field ($H \leq 5$ kOe). Magnetization curves of ZnO Co #5 (dose II) scale very well with those of ZnO Co #1 (dose I). However, twofold increase of dose Φ_{Co} results in lower than proportional increase of magnetization. We observed $M(7\ \mathrm{T}) = 6.8 \times 10^{16}\ \mu_{\mathrm{B}}/\mathrm{cm}^2$ for $\Phi_{\mathrm{Co}} = 4 \times 10^{16}\ \mathrm{cm}^{-2}$, while $M(7\ \mathrm{T}) = 4.2 \times 10^{16}\ \mu_{\mathrm{B}}/\mathrm{cm}^2$ for $\Phi_{\mathrm{Co}} = 2 \times 10^{16}\ \mathrm{cm}^{-2}$. The magnetization of additional phase could be obtained for low temperatures by subtracting linear PM contribution. Unfortunately, practically it can be done for temperatures not higher than about 50 K for which PM magnetization can be considered as linear. Nevertheless, using the obtained M vs. H dependence at 50 K of the unknown phase, we have made the correction for the magnetization curves measured at $T = 2$, 5, 10, and 20 K. Magnetization dependence on magnetic field represented in M vs. H/T coordinates for these temperatures suggests weak antiferromagnetic interaction between Co ions. The corrected M vs. H at $T = 2$ K is well described by standard Brillouin function with $S = 2$. However, it should be borne in mind that for a small difference in samples centering in straw the magnetization data corrected by subtraction could be affected by some linear component.

Dependences of M vs. T measured at $H = 10$ kOe and $H = 1$ kOe for Co-implanted ZnO (ZnO Co #5 dose II) are depicted in Fig. 6a and b, respectively. In both figures magnetization of parent (not implanted reference samples) ZnO could be compared to the magnetization of relevant Co-implanted ZnO. The additional PM signal resultant from Co-implanted thin layer of ZnO is clearly seen at low temperatures. In the insets in Fig. 6a and b magnetizations of ZnO Co #5 after correction for magnetization of parent ZnO are shown. Dominating at low temperatures PM contribution is accompanied by contrary dominating for $T > 20$ K unknown pronounced slowly decreasing with increase of temperature contribution. The black line in Fig. 6a, inset, represents the Brillouin function with parameters obtained due to fitting of the corrected M vs. H curve (described above) at $T = 2$ K. Most probably this additional superparamagnetic phase originates from Co clusters.

4. Conclusions

For ZnO implanted with Co and noble gases Ar and Kr, a significant effect of implantation on magnetic properties was observed only in the case of cobalt. Importantly, the observed magnetization shows the saturation effect. We observed $M(7\ \mathrm{T}) = 6.8 \times 10^{16}\ \mu_{\mathrm{B}}/\mathrm{cm}^2$ for $\Phi_{\mathrm{Co}} = 4 \times 10^{16}\ \mathrm{cm}^{-2}$ while $M(7\ \mathrm{T}) = 4.2 \times 10^{16}\ \mu_{\mathrm{B}}/\mathrm{cm}^2$ for $\Phi_{\mathrm{Co}} = 2 \times 10^{16}\ \mathrm{cm}^{-2}$.

References

[1] S. Mal, S. Nori, J. Narayan, J.T. Prater, D.K. Avasthi, *Acta Mater.* **61**, 2763 (2013).

[2] A.S. Fedorov, M.A. Visotin, A.S. Kholtobina, A.A. Kuzubov, N.S. Mikhaleva, H.S. Hsu, *J. Magn. Magn. Mater.* **440**, 5 (2017).

[3] L.M.C. Pereira, J.P. Araújo, U. Wahl, S. Decoster, M.J. Van Bael, K. Temst, A. Vantomme, *J. Appl. Phys.* **113**, 023903 (2013).

[4] J.J. Lee, G.Z. Xing, J.B. Yi, T. Chen, M. Ionescu, S. Li, *Appl. Phys. Lett.* **104**, 012405 (2014).

[5] Y. Huang, W. Zhou, P. Wu, *Solid State Commun.* **183**, 31 (2014).

[6] M. Xu, H. Yuan, B. You, P.F. Zhou, C.J. Dong, M.Y. Duan, *J. Appl. Phys.* **115**, 093503 (2014).

[7] Z. Werner, J. Gosk, A. Twardowski, M. Barlak, C. Pochrybniak, *Nucl. Instrum. Methods Phys. Res. B* **358**, 174 (2015).

[8] University of Surrey, SUSPRE.